

# Copper-mediated formation of hydrogen peroxide from the amylin peptide: A novel mechanism for degeneration of islet cells in type-2 diabetes mellitus?

Atef Masad<sup>a</sup>, Lee Hayes<sup>a</sup>, Brian J. Tabner<sup>a</sup>, Stuart Turnbull<sup>a</sup>, Leanne J. Cooper<sup>a</sup>, Nigel J. Fullwood<sup>a</sup>, Matthew J. German<sup>b</sup>, Fuyuki Kametani<sup>c</sup>, Omar M.A. El-Agnaf<sup>d</sup>, David Allsop<sup>a,\*</sup>

<sup>a</sup> Biomedical Sciences Unit, Department of Biological Sciences, Lancaster University, Lancaster LA1 4YQ, UK

<sup>b</sup> School of Dental Sciences, University of Newcastle, Newcastle upon Tyne NE2 4BW, UK

<sup>c</sup> Department of Molecular Neurobiology, Tokyo Institute of Psychiatry, 2-1-8 Kamikitazawa, Setagayaku, Tokyo 156-8585, Japan

<sup>d</sup> Department of Biochemistry, United Arab Emirates University, Al-Ain 17666, United Arab Emirates

Received 18 June 2007; accepted 24 June 2007

Available online 2 July 2007

Edited by Barry Halliwell

**Abstract** Amyloid deposits derived from the amylin peptide accumulate within pancreatic islet  $\beta$ -cells in most cases of type-2 diabetes mellitus (T2Dm). Human amylin ‘oligomers’ are toxic to these cells. Using two different experimental techniques, we found that  $H_2O_2$  was generated during the aggregation of human amylin into amyloid fibrils. This process was greatly stimulated by Cu(II) ions, and human amylin was retained on a copper affinity column. In contrast, rodent amylin, which is not toxic, failed to generate any  $H_2O_2$  and did not interact with copper. We conclude that the formation of  $H_2O_2$  from amylin could contribute to the progressive degeneration of islet cells in T2Dm.

© 2007 Federation of European Biochemical Societies. Published by Elsevier B.V. All rights reserved.

**Keywords:** Type-2 diabetes; Amylin; Hydrogen peroxide; Electron spin resonance; Amplex red; Copper

## 1. Introduction

Type-2 diabetes mellitus (T2Dm) is an incurable disease that is characterized by hyperglycaemia arising from defects in both insulin action at responsive tissues and insulin secretion from  $\beta$ -cells in the pancreatic islets of Langerhans. Amyloid deposits are found in islet  $\beta$ -cells in up to 90% of patients with T2Dm [1]. They are derived from a peptide hormone called amylin [2] (or, alternatively, islet amyloid polypeptide [3]) that is made and co-secreted along with insulin [1]. In T2Dm, the levels of amylin are raised in parallel with the increased demand for

insulin, and this is thought to induce concentration-dependent amylin aggregation [1]. Islet amyloid formation is associated with reduced  $\beta$ -cell mass [4] and human amylin ‘oligomers’ (small, soluble aggregates) are toxic to cultured islet cells [5,6], suggesting that they could contribute to progressive islet  $\beta$ -cell failure. Amylin oligomers can disrupt membranes [7,8] and inflict oxidative damage to cells [9], but the precise molecular mechanisms responsible for these effects have not been established.

The A $\beta$  peptide, which accumulates at the centre of senile plaques in the brain in Alzheimer’s disease (AD), can generate  $H_2O_2$  directly from molecular oxygen, apparently *via* electron-transfer reactions involving bound redox-active transition metal ions (Fe and Cu) [10].  $H_2O_2$  is itself toxic to cells, but, if formed in the vicinity of redox-active metal ions, such as Fe(II), is readily converted into hydroxyl radicals, *via* Fenton’s reaction. These highly reactive radicals can induce damaging oxidation, cell toxicity and cell death.

Here, we show that the human amylin peptide also has the ability to generate  $H_2O_2$  during amyloid fibril formation *in vitro*, and that this process is greatly stimulated by Cu(II) ions.

## 2. Materials and methods

### 2.1. Synthetic peptides

Human amylin (amide) (hA) (Fig. 1) was purchased from American Peptide Company, Sunnyvale, CA, USA. Its purity was 93.3% as determined by high-performance liquid chromatography mass spectroscopic analysis. The equivalent rodent amylin peptide (rA) (Fig. 1) was purchased from the same source (purity 99%).

The A $\beta$ (1–40) and A $\beta$ (1–42) peptides were synthesised on a Milligen 9050 peptide synthesiser as described in detail elsewhere [11]. The control peptides A $\beta$ (40–1) (reverse) and A $\beta$ (1–40)Met<sup>35</sup>Nle were from Biosource International (Belgium).

### 2.2. Amplex Red assay

Amplex Red (10-acetyl-3,7-dihydroxyphenoxazine) is a non-fluorescent compound that is oxidised by  $H_2O_2$  in the presence of horseradish peroxidase (HRP) to yield the highly fluorescent product, resorufin [12]. Both the A $\beta$  and amylin peptides were incubated at 100  $\mu$ M in 50 mM Na phosphate, 0.14 M NaCl, pH 7.4 (PBS) at 37 °C for selected time periods before testing for  $H_2O_2$  formation. For the Amplex Red assays, a 10 mM stock solution of Amplex Red was prepared in

\*Corresponding author. Fax: +44 1524 593192.

E-mail address: d.allsop@lancaster.ac.uk (D. Allsop).

**Abbreviations:** A $\beta$ , amyloid  $\beta$ -peptide; AD, Alzheimer’s disease; AFM, atomic force microscopy; DETAPAC, diethylenetriaminepentaacetic acid; DMPO, 5,5-dimethyl-1-pyrroline *N*-oxide; DMPO-OH, DMPO hydroxyl radical adduct; DMSO, dimethyl sulfoxide; EM, electron microscopy; ESR, electron spin resonance; hA, human amylin; HRP, horseradish peroxidase; PBS, phosphate-buffered saline; rA, rodent amylin; SDS-PAGE, sodium dodecyl sulfate–polyacrylamide gel electrophoresis; T2Dm, type-2 diabetes mellitus

1                    10                    20                    30                    37  
 hA KCNTATCATQRLANFLVHSSNNF**G**AILLSSTNVGSNTY-NH<sub>2</sub>  
 rA KCNTATCATQRLANFLV**R**SSNNL**G**PVLP**P**TNVGSNTY-NH<sub>2</sub>

Fig. 1. Amylin peptides employed for this study. Amino acid differences between human amylin (hA) and rodent amylin (rA) are underlined.

dimethyl sulfoxide (DMSO) and a HRP stock solution (10 U/ml) was prepared in phosphate-buffered saline (PBS) (both stored at  $-20^{\circ}\text{C}$ ). To produce the Amplex Red working solution, the stock HRP was diluted 1/1000 in PBS and this diluted HRP solution (100  $\mu\text{l}$ ) and Amplex Red stock solution (50  $\mu\text{l}$ ) were added to 4.85 ml of PBS. Standard curves were obtained using H<sub>2</sub>O<sub>2</sub> solutions with concentrations ranging from 0.05 to 1.0  $\mu\text{M}$ . For the assay, a 10  $\mu\text{l}$  sample of standard H<sub>2</sub>O<sub>2</sub> solution, or test sample, was added to each well of a black, flat-bottomed, 384-well microtitre plate (Nunc), in triplicate, and then 10  $\mu\text{l}$  of Amplex Red working solution was added. Similar results were obtained with 50  $\mu\text{l}$  samples plus 50  $\mu\text{l}$  Amplex Red working solution, in 96-well plates. Fluorescence of the resorufin product was read, after 30 min incubation at room temperature, on a Victor<sup>2</sup> 1420 plate reader, with  $\lambda_{\text{Ex}} = 544 \text{ nm}$  and  $\lambda_{\text{Em}} = 590 \text{ nm}$ . Solutions containing no H<sub>2</sub>O<sub>2</sub> were used as a measure of background fluorescence, which was subtracted from all values.

In some experiments, catalase (1000 U/ml) was added to the peptide samples at the end of their incubation period, before they were added to the Amplex Red working solution. In others, the metal ion chelator diethylenetriaminepentaacetic acid (DETAPAC) (100  $\mu\text{M}$ ) was added prior to incubation of the peptide solutions.

To study the effects of metal ions, hA (100  $\mu\text{M}$ ) was incubated for various times at  $37^{\circ}\text{C}$  in the presence of 10  $\mu\text{M}$  of each of the following: CuCl<sub>2</sub>, ZnCl<sub>2</sub>, FeCl<sub>3</sub>, AlCl<sub>3</sub>, MgCl<sub>2</sub>; rA was incubated with 10  $\mu\text{M}$  CuCl<sub>2</sub> as a control. In these experiments, HEPES buffer (10 mM *N*-2-hydroxyethylpiperazine-*N'*-2-ethanesulfonic acid, pH 7.4) was used in all treatments (including controls) instead of PBS. The samples were then tested using the Amplex Red method.

### 2.3. Electron spin resonance (ESR) spectroscopy

The hydroxyl radical was formed (*via* Fenton chemistry) from any H<sub>2</sub>O<sub>2</sub> generated during incubation of the required peptide at 100  $\mu\text{M}$  in PBS, at  $37^{\circ}\text{C}$  and detected by ESR spectroscopy, as described previously [13–15]. The method employed the reaction of this radical with the spin trap 5,5-dimethyl-1-pyrroline *N*-oxide (DMPO) to form the hydroxyl radical adduct (DMPO-OH), which has a uniquely characteristic 4-line ESR spectrum with  $a(\text{N})$  1.50 and  $a(\text{H}_{\beta})$  1.46 mT [13–15]. Samples of the required peptide (50  $\mu\text{l}$ ), incubated both in the absence and presence of various metal ions (2  $\mu\text{M}$ ), were withdrawn at selected time-points for ESR analysis.

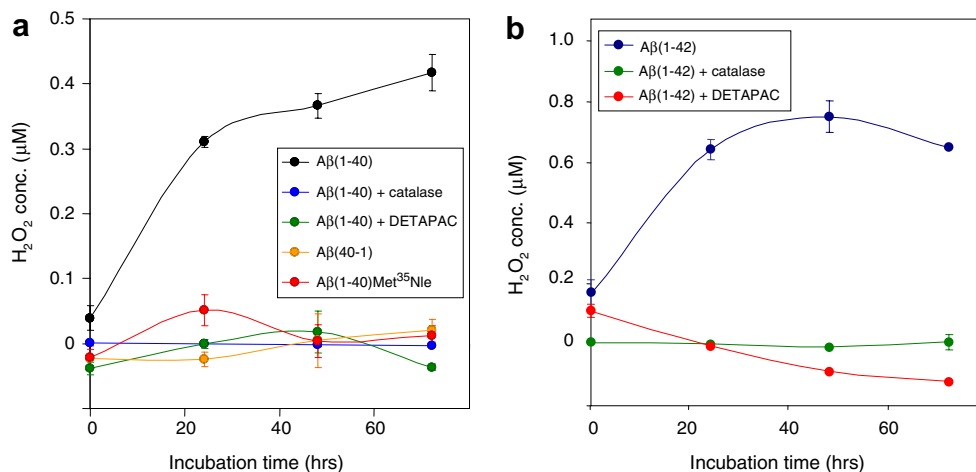


Fig. 2. Results for A $\beta$ , employing the Amplex Red method. (a) A $\beta$ (1–40) incubated with and without catalase or DETAPAC, compared with A $\beta$ (40–1) and A $\beta$ (1–40)Met<sup>35</sup>Nle; (b) A $\beta$ (1–42) incubated with and without catalase or DETAPAC.

### 2.4. Atomic force microscopy

Samples selected for analysis by atomic force microscopy (AFM) at various time points were diluted 5 times in MQ water prior to imaging. The diluted samples (1  $\mu\text{l}$ ) were applied to freshly cleaved mica-covered metal sample stubs and air dried. AFM imaging was undertaken using a Multimode AFM with a Nanoscope IIIa controller in tapping mode in air with Si<sub>3</sub>N<sub>4</sub> high spring constant cantilevers (TESP, Veeco, Cambridge, UK). A high-resolution scanner (E-type scanner, Veeco) was used to allow the best possible resolution of deposits at early incubation times. Five randomly chosen areas were imaged on each sample and the subsequent images were then carefully analyzed for ultrastructural differences.

### 2.5. Transmission electron microscopy

Samples of incubated peptides were selected for analysis by electron microscopy (EM) at various time points. They were applied to Formvar-coated nickel grids for 2 min and air dried prior to negative staining with 2% (w/v) uranyl acetate for 30 s and wicked using filter paper. The samples were air-dried and examined on a JEOL 1010 TEM.

### 2.6. Immobilised metal affinity chromatography

HiTrap chelating columns (Amersham Biosciences, 1 ml) were charged with either 0.1 M Cu(II) chloride or 0.1 M Fe(III) chloride and then washed with 5 ml of MQ water and 10 ml of 20 mM sodium phosphate, 0.5 M NaCl, pH 8 (metal-binding buffer) to remove excess metal ions. hA or rA (100  $\mu\text{g}/\text{ml}$  in metal binding buffer) were then loaded onto the columns. The peptides were eluted by using several 'stepwise' concentrations of imidazole (from 0 to 100 mM in metal binding buffer). The fractions from the columns were analyzed by 4–20% Tris–Glycine sodium dodecyl sulfate–polyacrylamide gel electrophoresis (SDS–PAGE).

## 3. Results

We used two quite independent methods in order to determine if synthetic human amylin peptide (hA), or the equivalent non-amyloidogenic and non-toxic rodent amylin peptide (rA), can generate H<sub>2</sub>O<sub>2</sub> during incubation *in vitro*. The first method employed the dye Amplex Red [12], whereas the second method was based on our previously published ESR spectroscopy technique [13–15]. We also examined the time period during which any H<sub>2</sub>O<sub>2</sub> was formed. The ultrastructure of the peptide aggregates was assessed from a study of AFM and EM images.

### 3.1. Amplex Red assays

We initially carried out experiments with A $\beta$ (1–40), A $\beta$ (1–42) and related control peptides to validate the Amplex Red method. These peptides were incubated at 100  $\mu$ M in PBS at 37 °C and samples were taken at various times for H<sub>2</sub>O<sub>2</sub> assay. An Amplex Red signal, which increased rapidly during the early course of aggregation, was detected from both A $\beta$ (1–40) and A $\beta$ (1–42) (Fig. 2). Overall, these results were compatible with our published ESR data showing that H<sub>2</sub>O<sub>2</sub> is generated during the early stages of A $\beta$  aggregation [16]. Inclusion of catalase at the end of the peptide incubation period blocked the Amplex Red signal, as did the presence during incubation of the metal-ion chelator DETAPAC. A $\beta$ (1–40)Met<sup>35</sup>Nle and A $\beta$ (40–1) (reverse peptide), both of which have been shown previously not to generate H<sub>2</sub>O<sub>2</sub> [17], failed to produce any signal in the Amplex Red assay.

We then proceeded to measure the levels of H<sub>2</sub>O<sub>2</sub> in similarly incubated solutions of hA and rA. In the case of hA, H<sub>2</sub>O<sub>2</sub> formation was detected during the course of peptide aggregation, reaching a maximum at around 72 h incubation time, before declining to background levels at longer incubation times (Fig. 3a). In contrast no H<sub>2</sub>O<sub>2</sub> was detected during the incubation of rA. The rate of decay of the H<sub>2</sub>O<sub>2</sub> self-generated from hA, and hence its stability, depends upon two factors. Firstly, direct reaction with the peptide and, secondly, on the availability of metal ions to convert it to hydroxyl radicals. A classic example of the differences in this rate of decay can be found when comparing H<sub>2</sub>O<sub>2</sub> levels generated by A $\beta$  (slow decay) with those from ABri (rapid decay) [16].

Freshly dissolved hA peptide showed no clear structures (Fig. 4a) but analysis of EM and AFM images obtained during the early stages of H<sub>2</sub>O<sub>2</sub> formation (3–6 h) revealed the presence of numerous short ‘protofibrils’ (Fig. 4b and c) whereas samples examined after prolonged incubation periods (24–72 h) revealed the presence of longer amyloid fibrils (Fig. 4d). The peroxide was, therefore, generated during amyloid fibril formation. The AFM images of the protofibrils formed from hA (Fig. 4c) were similar in appearance to those observed with A $\beta$  [16]. When hA was incubated in the presence

of various metal ions, only Cu(II) stimulated the formation of H<sub>2</sub>O<sub>2</sub> to any great extent (Fig. 3b). In the presence of Cu(II), the Amplex Red signal from hA again reached a peak at around 72 h incubation time, but there was a 6-fold increase in H<sub>2</sub>O<sub>2</sub> levels compared with those obtained from hA alone. The ultrastructural appearance of the hA aggregates formed during incubation, or the aggregation time, did not appear to be markedly changed by the presence of Cu(II) ions (Fig. 4e and f). It should be noted that no distinct fibrils were observed with rA incubated with or without Cu(II) ions.

In all of these experiments, any positive signal from hA was always blocked by the addition of catalase at the end of the peptide incubation period (confirming the detection of H<sub>2</sub>O<sub>2</sub>) or by the inclusion of DETAPAC during peptide incubation (suggesting that metal ions are involved) (Fig. 3a). The presence of Cu(II) ions during the incubation of rA failed to stimulate the formation of H<sub>2</sub>O<sub>2</sub> (Fig. 3b).

### 3.2. ESR measurements

For the ESR method, hA was incubated (as before) in the presence or absence of various metal ions, and any H<sub>2</sub>O<sub>2</sub> formed was detected by its conversion into hydroxyl radicals, which were trapped with DMPO [13–15]. A weak 4-line spectrum corresponding to the hydroxyl radical adduct was often observed without added metal ions, but this was sometimes absent altogether (Fig. 5a). However, the intensity of this spectrum was greatly enhanced when hA was co-incubated with Cu(II) ions (Fig. 5b). All of the ESR spectra obtained from hA could be blocked with catalase (Fig. 5c) or DETAPAC (Fig. 5d) and no spectra were observed under any conditions from rA (Fig. 5e).

### 3.3. Copper ion binding to hA

hA was retained on a HiTrap metal-chelating column charged with Cu(II) ions and could be subsequently eluted with 25 mM (but not 10 mM) imidazole (Fig. 6a). This peptide failed to bind to a similar column charged with Fe(III) ions (Fig. 6b). Furthermore, rA did not bind to either of these metal-loaded Hitrap columns (Fig. 6c).

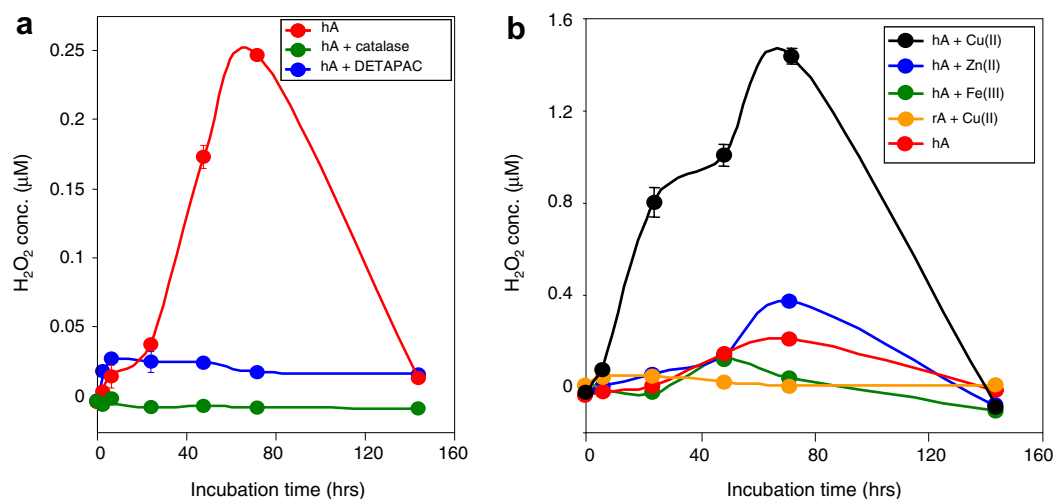


Fig. 3. Results for amylin, employing the Amplex Red method. (a) hA, with and without catalase or DETAPAC; (b) effects of metal ions (10  $\mu$ M) on hA and rA. In addition to those shown, Al(III) and Mn(II) had no significant effect on the Amplex Red signal from hA.

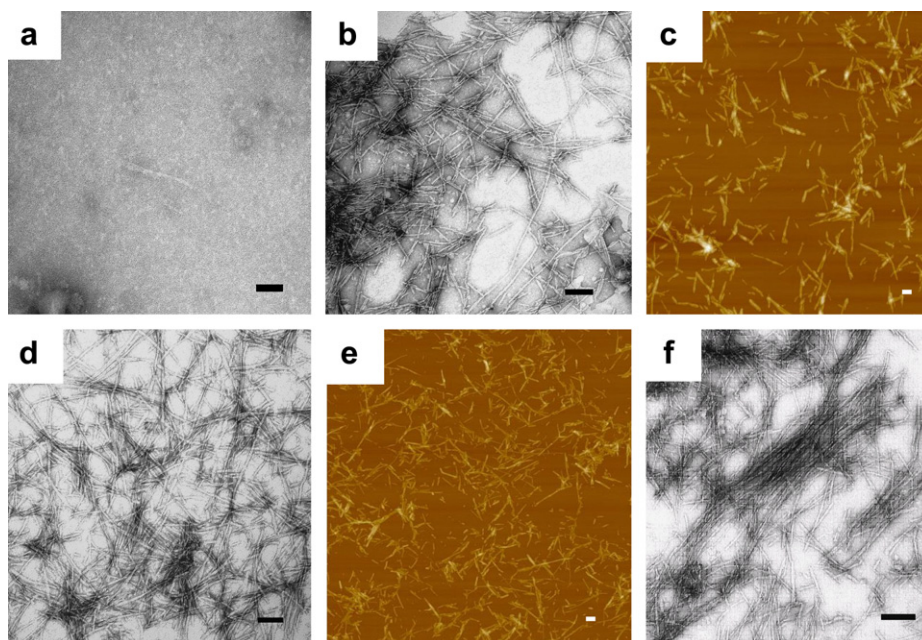


Fig. 4. Ultrastructural appearance of hA aggregates. (a) EM image at zero incubation time; (b) EM image of 'protofibrils' at 6 h incubation; (c) AFM image of 'protofibrils' at 6 h incubation; (d) EM image of fully-formed amyloid fibrils at 72 h; (e) AFM image at 3 h incubation, in the presence of Cu(II); (f) EM image at 72 h incubation, in the presence of Cu(II).

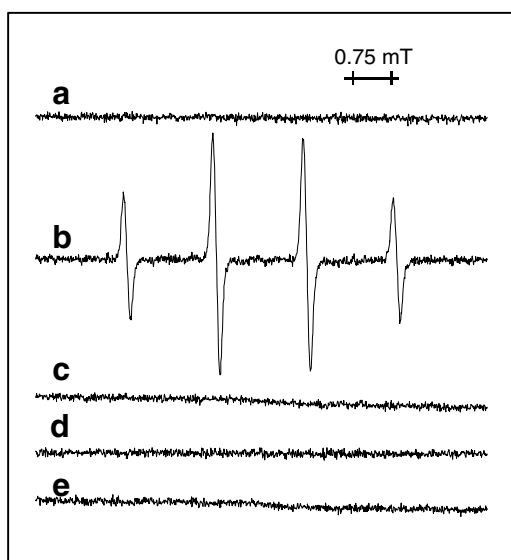


Fig. 5. ESR spectra recorded from amylin peptides. (a) hA; (b) is (a) incubated in the presence of Cu(II) (2  $\mu$ M); (c) is (b) incubated in the presence of catalase; (d) is (b) incubated in the presence of DETAPAC; (e) rA incubated in the presence of Cu(II) (2  $\mu$ M). A control experiment containing no peptide gave spectra similar to those shown in (a), (c), (d) and (e).

#### 4. Discussion

Although it has been established previously that exposure to the hA peptide increases  $H_2O_2$  levels in cultured cells [18], our results, employing two completely independent techniques (i.e., Amplex Red and ESR spectroscopy), demonstrate, for the first time, that  $H_2O_2$  is generated directly during the aggregation of hA in vitro, and also that the formation of  $H_2O_2$  in

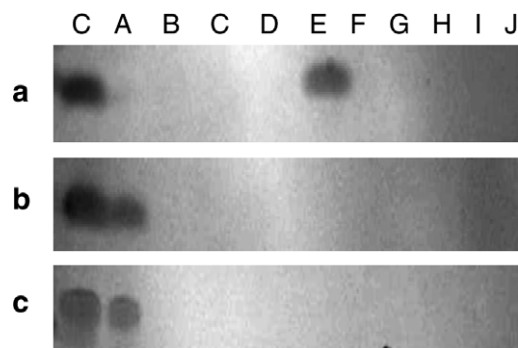


Fig. 6. Elution of amylin from metal-loaded HiTrap columns. (a) hA binds to Cu(II) and is eluted with 25 mM imidazole: C = hA control; A,B = 0 mM imidazole; C,D = 10 mM imidazole; E,F = 25 mM imidazole; G,H = 50 mM imidazole; I,J = 100 mM imidazole. (b) hA fails to bind to Fe(III) and is eluted with the first wash: lanes as before; (c) rA fails to bind to Cu(II): lanes as before.

this way is selectively stimulated by Cu(II) ions. The accumulation of  $H_2O_2$  was confirmed by the experiments with catalase, which blocked both of the Amplex Red and ESR signals. Similar experiments with DETAPAC suggest the involvement of metal ions, even when these are not added externally to the peptide.

The demonstration of an interaction between hA and the copper-loaded HiTrap columns suggests a mechanism for the generation of hydrogen peroxide involving the binding of Cu(II) ions to hA. This would potentially result in the formation of a redox-active complex. The donation of electrons from the peptide to Cu(II) ions would result in the formation of a Cu(I)-peptide complex, which could also be formed by the direct binding of the peptide to Cu(I) ions. The Cu(I)-complex could stimulate the formation of  $H_2O_2$  from  $O_2$  and result in



a consequent return to the Cu(II) oxidation state. Subsequent cycling of this redox system could occur, resulting in the generation of hydroxyl radicals from H<sub>2</sub>O<sub>2</sub> via Fenton chemistry.

The formation of H<sub>2</sub>O<sub>2</sub> from hA by this type of mechanism could explain the well-established toxicity of this peptide towards cultured islet cells. This would be in accord with previous reports that the cytotoxicity induced by hA involves oxidative damage [9] and can be reduced by anti-oxidants [19]. The ready formation of hydroxyl radicals from H<sub>2</sub>O<sub>2</sub> in the presence of redox-active transition metal ions could also contribute towards *in vivo* damage to the pancreas in T2Dm, for which there is extensive evidence for the involvement of reactive oxygen species [1].

Our results also add weight to the emerging hypothesis that oxidative damage during early oligomer formation could represent a common mechanism of toxicity for many amyloidogenic proteins and peptides [8,13–17,20]. This hypothesis is further supported by the fact that rA, which is not toxic to cells [21,22], failed to generate any H<sub>2</sub>O<sub>2</sub> in our experiments, presumably due to its inability to aggregate and/or to interact with copper ions.

A possible role for copper ions in T2Dm has already been implied by the finding that the level of copper is significantly higher (while those of zinc and magnesium are lower) in serum from diabetic patients than controls [23]. This suggests that copper could play an important role in the pathogenesis of T2Dm, possibly including the facilitation of H<sub>2</sub>O<sub>2</sub> generation from amylin, and, ultimately in the degeneration and death of pancreatic islet cells. Our data provide a new rationale and added impetus for the clinical use of copper chelators in T2Dm [24] as well as opening up additional avenues of research into the etiology, pathogenesis and treatment of this disease.

*Acknowledgements:* We thank The Ford Foundation (USA) for an International Postgraduate Research Studentship (to A.M.) and The Wellcome Trust for a Project Grant (GR065764AIA).

## References

- [1] Höppener, J.W. and Lips, C.J.M. (2006) Role of islet amyloid in type 2 diabetes mellitus. *Int. J. Biochem. Cell Biol.* 38, 726–736.
- [2] Cooper, G.J.S., Willis, A.C., Clark, A., Turner, R.C., Sim, R.B. and Reid, K.B.M. (1987) Purification and characterization of a peptide from amyloid-rich pancreases of type 2 diabetic patients. *Proc. Natl. Acad. Sci. USA* 84, 8628–8632.
- [3] Westermark, P., Wernstedt, C., Wilander, E., Hayden, D.W., O'Brien, T.D. and Johnson, K.H. (1987) Amyloid fibrils in human insulinoma and islets of langerhans of the diabetic cat are derived from a neuropeptide-like protein also present in normal islets. *Proc. Natl. Acad. Sci. USA* 84, 3881–3885.
- [4] De Koning, E.J., Bodkin, N.L., Hansen, B.C. and Clark, A. (1993) Diabetes mellitus in Macaca mulatto monkeys is characterised by islet amyloidosis and reduction in beta cell population. *Diabetologia* 36, 378–384.
- [5] Konarkowska, B., Aitken, J.F., Kistler, J., Zhang, S. and Cooper, G.J. (2006) The aggregation potential of human amylin determines its cytotoxicity towards islet beta-cells. *FEBS J.* 273, 3614–3624.
- [6] Ritzel, R.A., Meier, J.J., Lin, C.-Y., Veldhuis, J.D. and Butler, P.C. (2007) Human islet amyloid polypeptide oligomers disrupt cell coupling, induce apoptosis, and impair insulin secretion in isolated human islets. *Diabetes* 56, 65–71.
- [7] Janson, J., Ashley, R.H., Harrison, D., McIntyre, S. and Butler, P.C. (1999) The mechanism of islet amyloid polypeptide toxicity is membrane disruption by intermediate-sized toxic amyloid particles. *Diabetes* 48, 491–498.
- [8] Kaye, R., Sokolov, Y., Edmonds, B., McIntyre, T.M., Milton, S.C., Hall, J.E. and Glabe, C.G. (2004) Permeabilization of lipid bilayers is a common confirmation-dependent activity of soluble oligomers in protein folding diseases. *J. Biol. Chem.* 279, 46363–46366.
- [9] Janciauskiene, S. and Ahrén, B. (2000) Fibrillar islet amyloid polypeptide differentially affects oxidative mechanisms and lipoprotein uptake in correlation with cytotoxicity in two insulin-producing cell lines. *Biochem. Biophys. Res. Commun.* 267, 619–625.
- [10] Huang, X.D., Atwood, C.S., Hartshorn, M.A., Multhaup, G., Goldstein, L.E., Scarpa, R.C., Cuajungco, M.P., Gray, D.N., Lim, J., Moir, R.D., Tanzi, R.E. and Bush, A.I. (1999) The A beta peptide of Alzheimer's disease directly produces hydrogen peroxide through metal ion reduction. *Biochemistry* 38, 7609–7616.
- [11] El-Agnaf, O.M.A., Goodwin, H., Sheridan, J.M., Frears, E.R. and Austen, B.M. (2000) Improved solid-phase syntheses of amyloid proteins associated with neurodegenerative diseases. *Protein Peptide Lett.* 7, 1–8.
- [12] Zhou, M., Diwu, Z., Panchuk-Voloshina, N. and Haugland, R.P. (1997) A stable nonfluorescent derivative of resorufin for the fluorometric determination of trace hydrogen peroxide: applications in detecting the activity of phagocyte NADPH oxidase and other oxidases. *Anal. Biochem.* 253, 162–168.
- [13] Turnbull, S., Tabner, B.J., El-Agnaf, O.M.A., Moore, S., Davies, Y. and Allsop, D. (2001)  $\alpha$ -Synuclein implicated in Parkinson's disease catalyses the formation of hydrogen peroxide *in vitro*. *Free Radical Biol. Med.* 30, 1163–1170.
- [14] Turnbull, S., Tabner, B.J., Brown, D.R. and Allsop, D. (2003) Generation of hydrogen peroxide from mutant forms of the prion protein fragment PrP121–231. *Biochemistry* 42, 7675–7681.
- [15] Turnbull, S., Tabner, B.J., Brown, D.R. and Allsop, D. (2003) Copper-dependent generation of hydrogen peroxide from the toxic prion protein fragment PrP106–126. *Neurosci. Lett.* 336, 159–162.
- [16] Tabner, B.J., El-Agnaf, O.M.A., Turnbull, S., German, M.J., Paleologou, K.E., Hayashi, Y., Cooper, L.J., Fullwood, N.J. and Allsop, D. (2005) Hydrogen peroxide is generated during the very early stages of aggregation of the amyloid peptides implicated in Alzheimer's disease and familial British dementia. *J. Biol. Chem.* 280, 35789–35792.
- [17] Turnbull, B.J., Tabner, S., Fullwood, N.J., German, M. and Allsop, D. (2005) The production of hydrogen peroxide during early-stage protein aggregation: a common pathological mechanism in different neurodegenerative diseases? *Biochem. Soc. Trans.* 33, 548–550.
- [18] Schubert, D., Behl, C., Lesley, R., Brack, A., Dargusch, R., Sagara, Y. and Kimura, H. (1995) Amyloid peptides are toxic via a common oxidative mechanism. *Proc. Natl. Acad. Sci. USA* 92, 1989–1993.
- [19] Konarkowska, B., Aitken, J.F., Kistler, J., Zhang, S. and Cooper, G.J. (2005) Thiol reducing compounds prevent human amylin-evoked cytotoxicity. *FEBS J.* 272, 4949–4959.
- [20] Tabner, B.J., Turnbull, S., El-Agnaf, O.M.A. and Allsop, D. (2002) Formation of hydrogen peroxide and hydroxyl radicals from A $\beta$  and  $\alpha$ -synuclein as a possible mechanism of cell death in Alzheimer's disease and Parkinson's disease. *Free Radical Biol. Med.* 32, 1076–1083.
- [21] Lorenzo, A., Razzaboni, B., Weir, G.C. and Yankner, B.A. (1994) Pancreatic islet cell toxicity of amylin associated with type-2 diabetes mellitus. *Nature* 368, 756–760.
- [22] Hiddinga, H.J. and Eberhardt, N.L. (1999) Intracellular amyloidogenesis by human islet amyloid polypeptide induces apoptosis in COS-1 cells. *Am. J. Pathol.* 154, 1077–1088.
- [23] Isbir, T., Tamer, L., Taylor, A. and Isbir, M. (1994) Zinc, copper and magnesium status in insulin-dependent diabetes. *Diabetes Res.* 26, 41–45.
- [24] Lu, J., Chan, Y.K., Gamble, G.D., Poppitt, S.D., Othman, A.A. and Cooper, G.T. (2007) Triethylenetetramine and metabolites: levels in relation to copper and zinc excretion in urine of healthy volunteers and type 2 diabetic patients. *Drug Metab. Dispos.* 35, 221–227.